ELEC-H401

Design and Simulation of a DVB-C Transmission Chain

Hadislam Satouev
Cédric Sipakam

Professor
François Horlin

Teaching Assistants
....
....

Academic Year
2024 - 2025

Faculty
Electrical Engineering

Contents

List of Figures

Introduction

This project focuses on designing and simulating a Digital Video Broadcasting Cable transmission chain using Matlab. The main goal is to model and analyze the components of a typical modem. The first part of this project includes establishing an optimal communication chain over an ideal Additive White Gaussian Noise channel, mapping the signal into symbols, Nyquist filtering, and evaluating the performance of the system through Bit Error Rate simulations for Quadrature Amplitude Modulation signals. The second part revolves around the design and assessment of time and frequency synchronization algorithms. This encompasses evaluating the impact of synchronization errors such as carrier phase and frequency offset and sample time shift. The algorithms used for this purpose are the Gardner Algorithm for time recovery, and a differential cross-correlator for joint frame and frequency acquisition. Afterwards, their effectiveness is demonstrated through convergence analysis and residual error evaluation (double check). The study also explores phase interpolation techniques to mitigate remaining phase drifts. Finally, the project aims to validate the simulated chain through real-life experimentation on a Hybrid Fiber-Coax setup using Adalm-Pluto hardware, and to compare the simulated performance with experimental observations.

1 Optimal Communication Chain over the Ideal Channel

Figure ?? shows the simulated DVB-C baseband communication chain. The transmitter generates bits, maps them to QAM symbols, upsamples, and shapes them with a half-root Nyquist filter. The receiver uses a matched filter, downsamples, and demapps symbols. LDPC coding is not implemented.

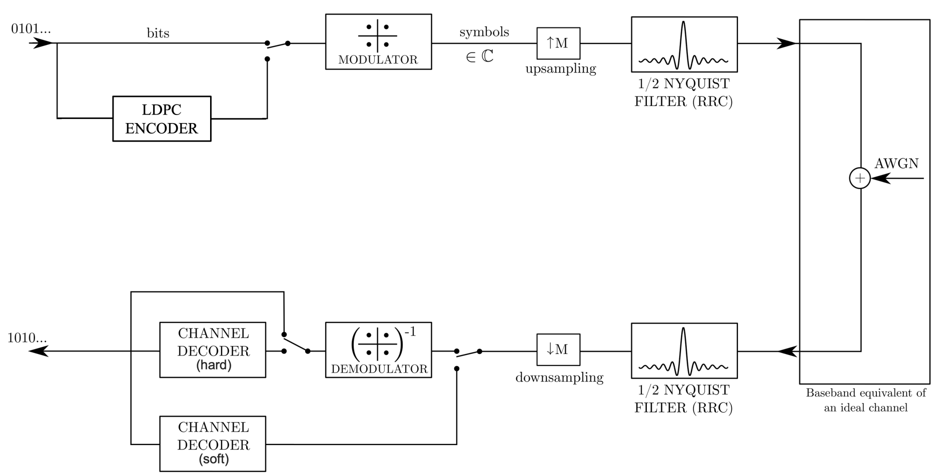

Figure 1: Block diagram of the communication system.

Symbol mapping transforms random bits into complex symbols. Demapping uses Maximum Likelihood (ML) to select the constellation symbol $\underline{s}_m$ minimizing Euclidean distance to the received sample $\underline{r}$:

$$\tilde{\underline{s}}_m^{ML} = \arg\min_{\underline{s}_m} \left(\sum_{k=1}^{K} (r_k - s_{mk})^2 \right) \tag{1}$$

This is equivalent to maximizing $\ln p(\underline{r}|\underline{s}_m)$ for an AWGN channel.

Nyquist filtering uses a root-raised cosine (RRC) filter $g(t)$ for pulse shaping and its matched version $g^*(-t)$ at the receiver. Their convolution $h(t) = g(t) \otimes g^*(-t)$ satisfies the Nyquist zero ISI criterion at T_{symb} intervals: $h(kT_{symb}) = \delta[k]$. The RRC frequency response $G(f) = \sqrt{H(f)}$, where $H(f)$ is the RC filter response:

$$H(f) = \begin{cases} T_{symb} & 0 \le |f| < \frac{1-\beta}{2T_{symb}} \\ \frac{T_{symb}}{2}\left(1 + \cos\left[\frac{\pi T_{symb}}{\beta}\left(|f| - \frac{1-\beta}{2T_{symb}}\right)\right]\right) & \frac{1-\beta}{2T_{symb}} \le |f| \le \frac{1+\beta}{2T_{symb}} \\ 0 & |f| > \frac{1+\beta}{2T_{symb}} \end{cases} \tag{2}$$

Figure **??** shows the simulated $H(f)$ for $R_{symb} = 5$ Msymb/s and $\beta = 0.2$, confining the signal to a 6 MHz bandwidth, and $h(t)$ illustrating ISI cancellation at kT_{symb}.

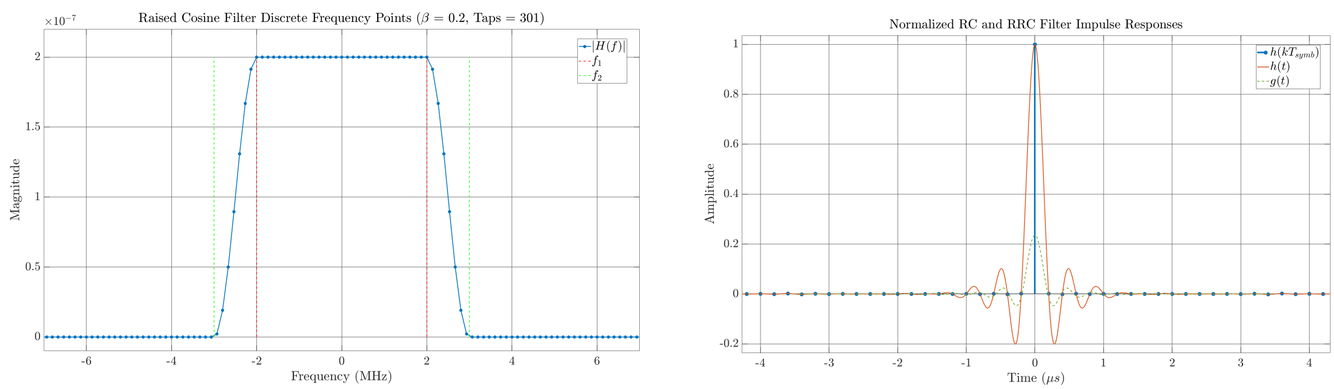

(a) RC Filter Frequency Response ($\beta = 0.2$).

(b) Normalized RC and RRC Impulse Responses.

Figure 2: Simulated Nyquist filter characteristics.

AWGN $n(t)$ is added to the signal $s(t)$, so $r(t) = s(t) + n(t)$. After matched filtering and sampling, $y[k] = I[k] + n_o[k]$, where $n_o[k]$ is complex Gaussian noise with variance $N_0/2$ per component. Performance is measured by BER vs. E_b/N_0. The theoretical P_b for M-QAM is:

$$P_b \approx \frac{4}{\log_2 M}\left(1 - \frac{1}{\sqrt{M}}\right) Q\left(\sqrt{\frac{3(\log_2 M)^2}{M-1}\frac{E_b}{N_0}}\right) \tag{3}$$

Figure **??** validates theoretical BER curves. Higher-order QAMs achieve higher data rates but require more power. Figure **??** shows the effect of AWGN on 16-QAM symbols before and after matched filtering, the latter showing tighter clusters due to SNR maximization.

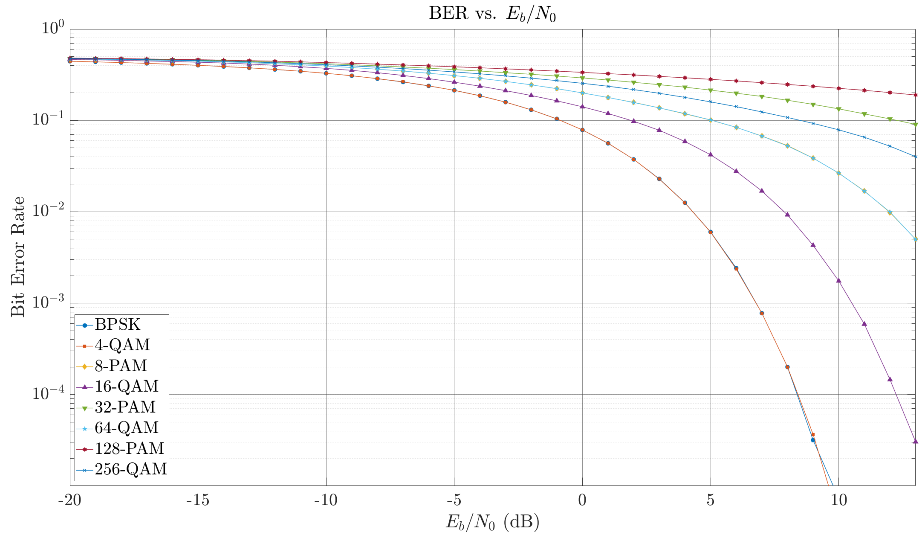

Figure 3: Simulated BER vs. E_b/N_0 for various modulation types.

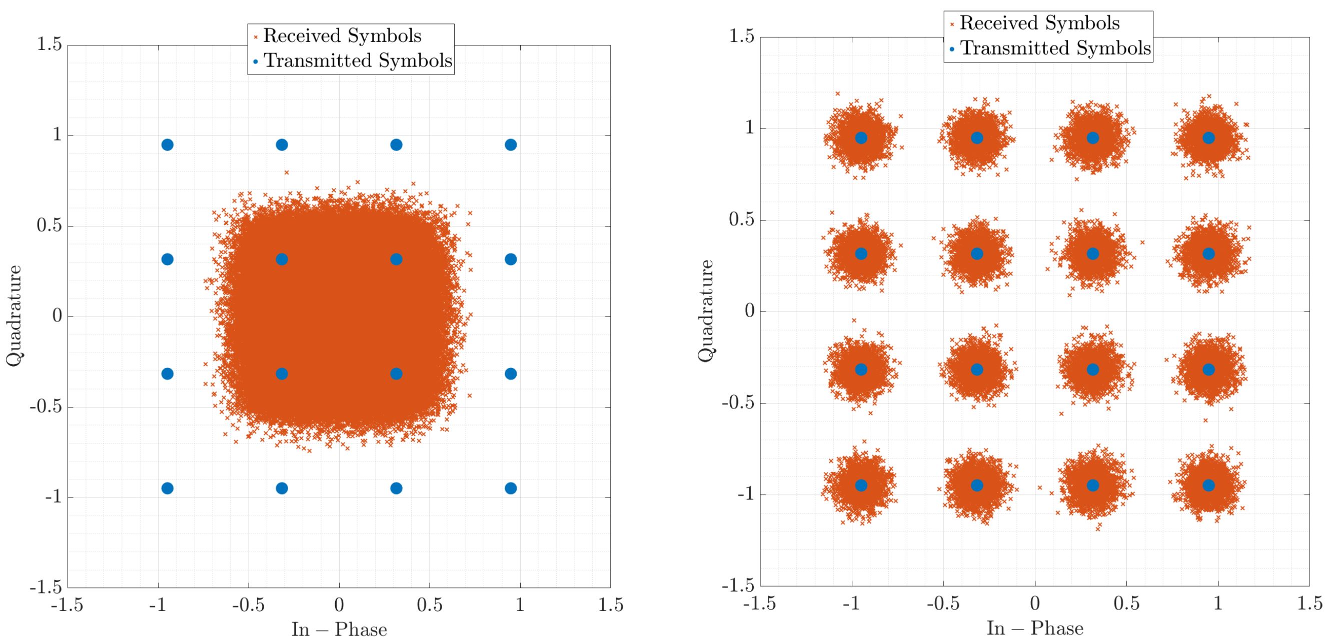

(a) Noisy 16-QAM before matched filter.

(b) 16-QAM after matched filtering.

Figure 4: Effect of AWGN and matched filtering on 16-QAM ($\frac{E_b}{N_0} = 15$ dB).

Questions: Optimal Communication Chain

vspace**Baseband vs. Bandpass Implementation:** Working with baseband equivalent models reduces complexity by avoiding high carrier frequencies, allowing lower simulation sampling rates and modular design of modulation/demodulation stages.

vspace

vspace**Sample Rate Selection:** The Matlab sampling rate F_s must be at least twice the maximum signal frequency F_{max} (Nyquist criterion) to prevent aliasing. For an RRC filter with roll-off β, $F_{max} = (1+\beta)/(2T_{symb})$. Thus, the oversampling factor M must ensure $F_s = M/T_{symb} \geq 2F_{max}$.

vspace

vspace**Simulating E_b/N_0 Ratio:** Noise power $P_n = N_0 F_s$. N_0 is derived from the target E_b/N_0 and calculated bit energy E_b. $E_b = E_s/\log_2(M)$, where E_s is average symbol energy. Complex noise $n(t) = \sqrt{P_n/2}(X + jY)$ is generated with $X, Y \sim \mathcal{N}(0,1)$.

vspace

vspace**Number and Length of Data Packets:** The number of bits per packet must be a multiple of $\log_2(M)$ for M-QAM to avoid unused bits. Total transmitted bits must be sufficient for statistically relevant BER estimation, typically such that at least 10-100 errors are observed for the target BER.

vspace**Supported Bit Rate vs. Physical Bandwidth:** The two-sided Nyquist bandwidth is $B = (1+\beta)/T_{symb}$. The bit rate $R_b = (\log_2 M)/T_{symb} = (\log_2 M) \cdot R_{symb}$. Thus $R_b = R_{symb} \cdot \log_2 M = \frac{B}{1+\beta} \log_2 M$.

vspace

vspace**Trade-off: Capacity vs. Reliability (Constellation Size):** Larger constellations (higher M) increase capacity (more bits/symbol, higher R_b for fixed bandwidth). However, constellation points are closer, reducing Euclidean distance and increasing susceptibility to noise, thus degrading BER for a given E_b/N_0 (lower reliability).

vspace

vspace**Choice of Half-Root Nyquist Filter:** RRC filters are used because: 1) When paired (transmitter and matched receiver filter), they form an overall Nyquist filter, ensuring zero ISI at correct sampling instants. 2) The matched filter maximizes SNR at the detector input. 3) They provide good spectral containment.

vspace

vspace**Optimal Demodulator Implementation:** The optimal demodulator for AWGN channels uses a filter matched to the transmitted pulse shape $g(t)$, i.e., $g^*(-t)$, followed by sampling at symbol instants kT_{symb}. This maximizes the output SNR.

vspace

vspace**Optimal Detector Implementation:** The optimal detector minimizes symbol error probability. For equiprobable symbols in AWGN, this corresponds to the Maximum Likelihood (ML) criterion: choose symbol s_m that maximizes $p(r|s_m)$. This simplifies to minimizing the Euclidean distance: $\hat{s}_{ML} = \arg\min_{s_m} ||r - s_m||^2$.

vspace

2 Time and Frequency Synchronization

Synchronization aligns receiver timing and carrier with the transmitter. Errors include Carrier Frequency Offset (Δf), Phase Offset (ϕ_0), and Sample Time Shift (t_0), illustrated in Figure **??**.

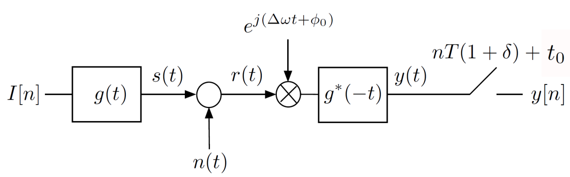

(a) Synchronization mismatches.

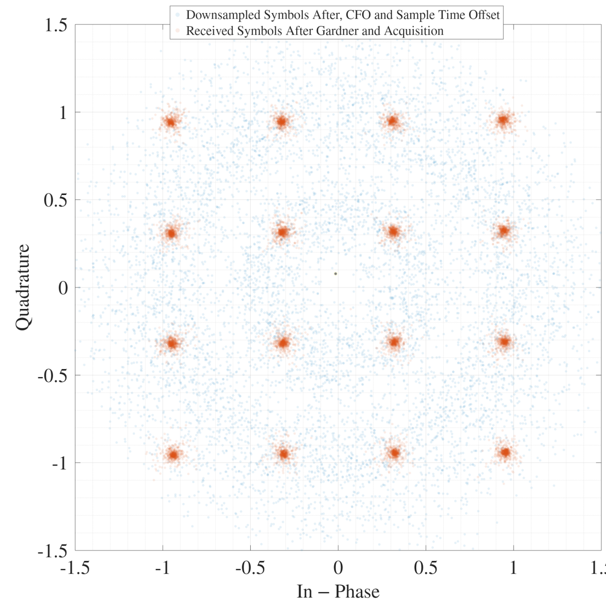

(b) 16-QAM: initial errors (blue) vs. post-sync (red).

Figure 5: Synchronization challenges and overall correction impact ($E_b/N_0 = 20$ dB for (b)).

Synchronization errors degrade performance. ϕ_0 rotates the constellation ($y[n] = I[n]e^{j\phi_0}$). Δf causes phase drift ($y[n] = I[n]e^{j(2\pi\Delta f n T_{symb}+\phi_0')}$) and ISI due to filter mismatch. t_0 causes attenuation and ISI: $y[n] = I[n]h(t_0) + \sum_{m\neq n} I[m]h((n-m)T_{symb}+t_0)$. Figures **??** and **??** show these impacts on BER and 16-QAM constellations.

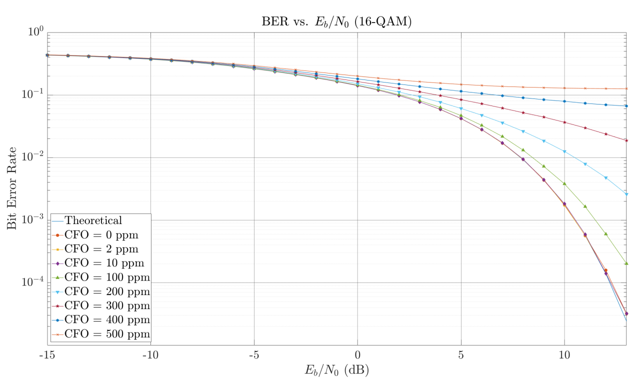

(a) BER vs. E_b/N_0 for varying CFO.

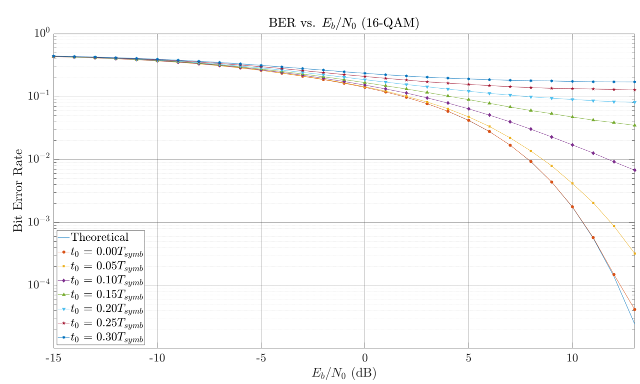

(b) BER vs. E_b/N_0 for varying t_0/T_{symb}.

Figure 6: Impact of CFO and timing errors on BER for 16-QAM.

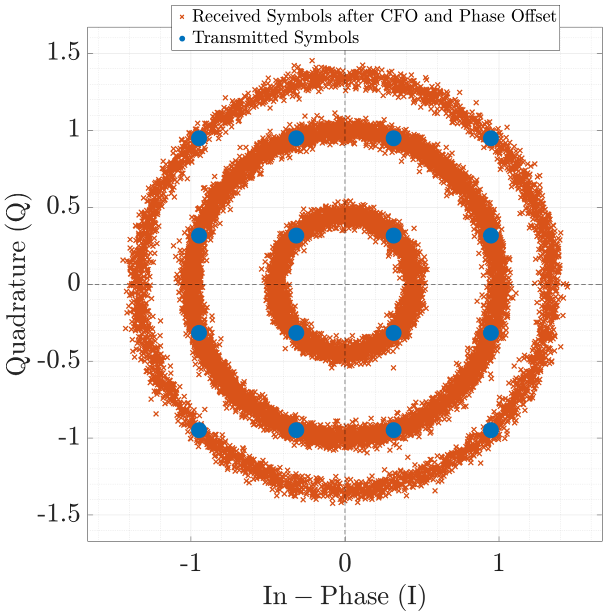

(a) Constellation with CFO and Phase Offset.

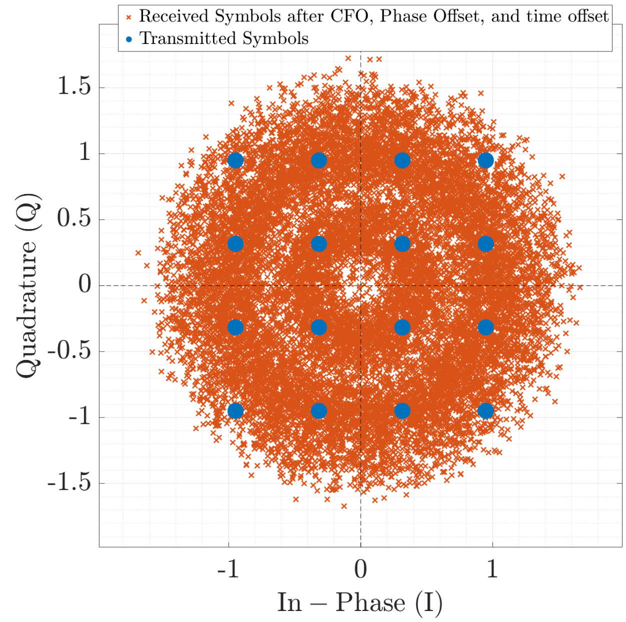

(b) Constellation with CFO, Phase Offset, and Time Offset.

Figure 7: Impact of synchronization errors on 16-QAM constellation ($E_b/N_0 = 20$ dB).

The Gardner algorithm, an NDA feedback loop, corrects sampling time errors $\epsilon[n]$. The update is:

$$\hat{\epsilon}[n+1] = \hat{\epsilon}[n] - \kappa \cdot \mathrm{Re}\left\{ y_{\hat{\epsilon}[n]}[n-1/2] \left(y^*_{\hat{\epsilon}[n]}[n] - y^*_{\hat{\epsilon}[n-1]}[n-1] \right) \right\} \tag{4}$$

Figure **??** (a) shows convergence for different loop gains κ, and (b) demonstrates robustness to CFO.

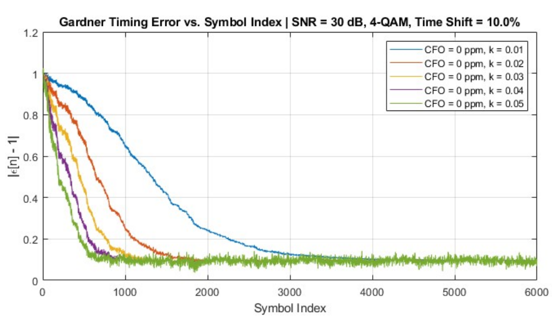

(a) Convergence for different κ.

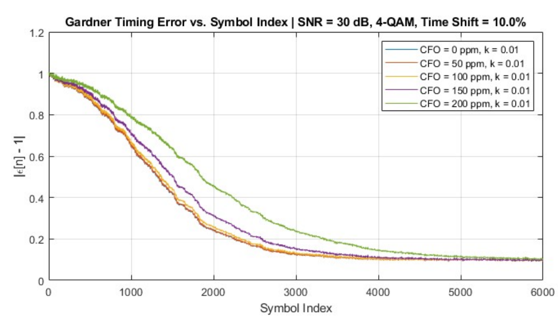

(b) Robustness to CFO.

Figure 8: Gardner algorithm performance: time error convergence.

Frame and coarse CFO acquisition use a DA differential cross-correlator with metric $D_k[n]$ from pilot $a[l]$:

$$D_k[n] = \frac{1}{N_p - k} \sum_{l=k}^{N_p-1} (y^*[n+l]a[l])(y^*[n+l-k]a[l-k])^* \tag{5}$$

Pilot start $\hat{n} = \arg\max_n \sum_{k=1}^{K_{avg}} |D_k[n]|$. CFO $\hat{\Delta f} = -\frac{1}{K_{avg}} \sum_{k=1}^{K_{avg}} \frac{\angle D_k[\hat{n}]}{2\pi k T_{symb}}$. Figures **??** and **??** show ToA and CFO estimation error standard deviations versus E_b/N_0 for varying pilot lengths N_p and averaging windows K_{avg}, respectively. Longer pilots and optimized K_{avg} improve accuracy.

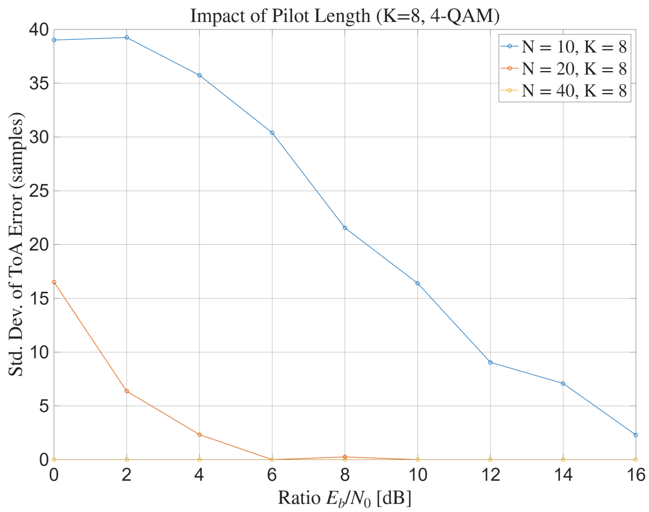

(a) ToA error std dev vs. N_p.

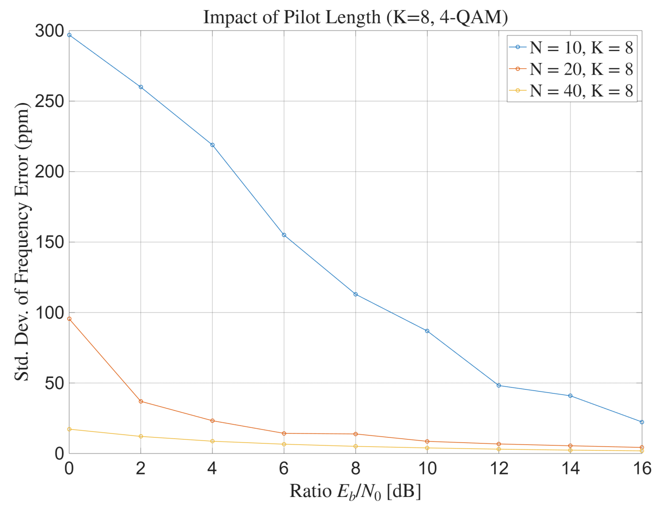

(b) CFO error std dev vs. N_p.

Figure 9: Acquisition error vs. E_b/N_0 for different pilot lengths (N_p).

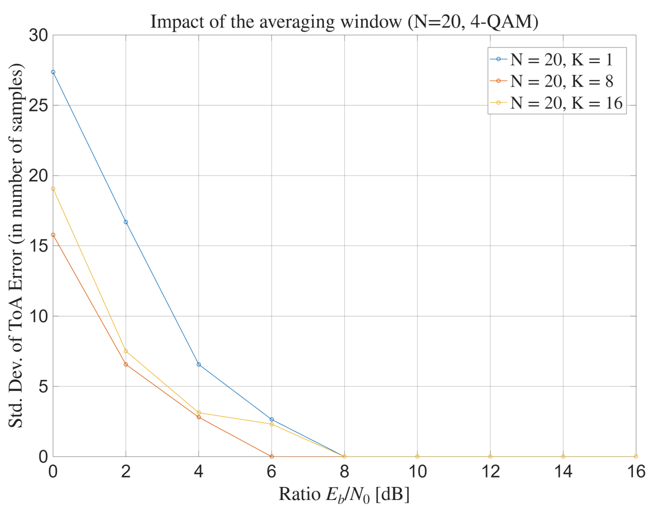

(a) ToA error std dev vs. K_{avg}.

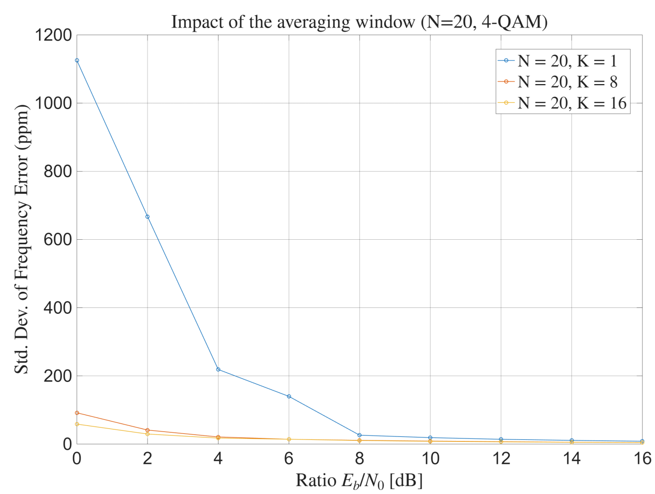

(b) CFO error std dev vs. K_{avg}.

Figure 10: Acquisition error vs. E_b/N_0 for different averaging windows (K_{avg}).

Residual phase error $\theta[n] = 2\pi\Delta f_{res} n T_{symb} + \phi_{res}$ after coarse CFO correction is handled by phase interpolation between pilot sequences. For a symbol at time t between pilots at $t_1(\hat{\theta}_1)$ and $t_2(\hat{\theta}_2)$, correction $\hat{\theta}(t) = \hat{\theta}_1 + (\hat{\theta}_2 - \hat{\theta}_1)\frac{t-t_1}{t_2-t_1}$. Figure **??** demonstrates this correction.

Images/phase_interp_constellation.png

Figure 11: QAM constellation: before (smeared) and after (tightened) phase interpolation.

The synchronization pipeline is: 1) Timing Recovery (Gardner), 2) Frame Acquisition, 3) Coarse CFO Acquisition, 4) Phase Interpolation. This order ensures robustness. Figure **??** (repeated in **??** for overview) visually confirms the significant improvement in constellation clarity after Gardner and Frame/CFO acquisition, crucial for reliable demodulation.

Questions: Time and Frequency Synchronization

vspace**Baseband Model with Synchronization Errors:** Received baseband signal $\tilde{r}_e(t) = \tilde{s}(t - \epsilon T_{symb} - t_0)e^{j(2\pi\Delta f t + \phi_0)}$, where $\tilde{s}(t)$ is ideal transmitted baseband signal, ϵ is normalized clock offset, t_0 time shift, Δf CFO, ϕ_0 phase offset. For sampling at $nT_{symb}(1+\delta) + t_0'$, considering $y[n]$ as output of matched filter and ADC.

vspace

vspace**Separating Phase Drift and ISI from CFO:** Phase drift from CFO is $e^{j2\pi\Delta f n T_{symb}}$ on symbols $I[n]$. ISI results from $g(t)e^{j2\pi\Delta f t}$ convolved with $g^*(-t)$ not being a perfect Nyquist pulse. To see ISI alone, multiply received symbols by $e^{-j2\pi\Delta f n T_{symb}}$ after matched filtering to remove coherent phase rotation, then observe BER degradation.

vspace

vspace**Simulating Sampling Time Shift:** Increase sampling rate by large factor M_{os} pre-filter. A shift of k samples at this high rate corresponds to $t_0 = k \cdot T_{symb}/M_{os}$. Alternatively, use interpolation on the oversampled signal at the receiver output to estimate values at $nT_{symb} + t_0$.

vspace

vspace**Selecting E_b/N_0 for Synchronization Tests:** E_b/N_0 must be high enough for synchronization algorithms to lock and provide meaningful performance metrics without being dominated by noise failures. Typically, choose values where uncoded BER is reasonably low (e.g., 10^{-2} to 10^{-4}), or a typical operating point. For some algorithms, a minimum E_b/N_0 (e.g., $>$ 4-6 dB) is needed for reliable acquisition, as seen in frame/frequency acquisition plots.

vspace

vspace**Selecting Pilot and Data Sequence Lengths:** Pilots (N_p): Long enough for accurate ToA/CFO/Phase estimation against noise (e.g., $N_p \geq 20{-}40$). Too short leads to high estimation variance. Data: Short enough between pilots to ensure phase drift from residual CFO is $< \pi$ (for unambiguous phase interpolation) and linear phase change assumption holds. Trade-off: Longer/more frequent pilots improve sync but reduce data throughput (overhead).

vspace

vspace**Order of Synchronization Operations:** 1. Timing Recovery (Gardner): Robust to CFO. 2. Frame/Frequency Acquisition (Differential Cross-correlator): Uses timed samples to find frame start and correct large CFO. 3. Phase Tracking/Interpolation: Corrects residual phase errors. This order allows each stage to operate on a signal pre-processed to mitigate errors that would impair its own performance.

vspace

vspace**Gardner Algorithm Error Computation and CFO Robustness:** Error: $e[n] = \mathrm{Re}\{y[n-1/2](y^*[n] - y^*[n-1])\}$. $y[n-1/2]$ is the mid-point sample. $(y^*[n] - y^*[n-1])$ estimates signal slope. If $y[n-1/2]$ and slope have same sign, timing is late; opposite sign, early. No transition means small slope, small update. Robustness to CFO: CFO causes phase rotation $\Delta\phi = 2\pi\Delta f T_{symb}$ between $y[n-1]$ and $y[n]$, and $\Delta\phi/2$ on $y[n-1/2]$. The error term uses $\mathrm{Re}\{\cdot\}$. For small $\Delta\phi$ per symbol (typical CFOs), $e^{j\Delta\phi} \approx 1 + j\Delta\phi$. The dominant terms in the error calculation are less affected by these small phase rotations.

vspace

vspace**Differential Cross-Correlator vs. Usual Cross-Correlator:** Usual cross-correlator ($C[n] = \sum y^*[n+l]a[l]$) is sensitive to CFO, as CFO rotates $y[n+l]$ causing phase terms $e^{j2\pi\Delta f(n+l)T_{symb}}$ that don't cancel in $|C[n]|$, degrading the peak. Differential cross-correlator (Eq. **??**) multiplies two correlation terms with a time lag k. The product $(y^*[n+l]a[l])(y[n+l-k]a^*[l-k])$ has phase $e^{-j2\pi\Delta f(n+l)T_{symb}} \cdot e^{j2\pi\Delta f(n+l-k)T_{symb}} = e^{-j2\pi\Delta f k T_{symb}}$. The phase is proportional to $k\Delta f$, allowing Δf estimation. The magnitude is less affected by the absolute phase. Summation for $k = 0$: $D_0[n] = \frac{1}{N_p}\sum |y[n+l]a[l]|^2$, which relates to energy detection but doesn't directly use the differential property for CFO estimation. The CFO estimation relies on $k \geq 1$.

vspace

vspace**Optimality of Frame/Frequency Acquisition Algorithms:** The ML criterion for joint ToA ($\hat{n}$) and CFO ($\Delta\omega$) estimation is $(\hat{n}, \Delta\omega) = \arg\max_{n,\omega} p(y[n]|a, \Delta\omega)$. Direct implementation is complex (2D search over n and ω). The differential cross-correlator is a near-optimal, lower-complexity approximation. It's not strictly ML optimal because it simplifies the likelihood function or uses derived metrics, often omitting terms like received signal power that an exact ML estimator might include.

vspace